

Optimization of PEM Fuel Cell Biphasic Model

Boubekeur Dokkar, Nasreddine Chennouf, Noureddine Settou, Belkhir Negrou, and Abdesslam Benmhidi

Abstract—The optimal operation of proton exchange membrane fuel cell (PEMFC) requires good water management which is presented under two forms vapor and liquid. Moreover, fuel cells have to reach higher output require integration of some accessories which need electrical power. In order to analyze fuel cells operation and different species transport phenomena a biphasic mathematical model is presented by governing equations set. The numerical solution of these conservation equations is calculated by Matlab program. A multi-criteria optimization with weighting between two opposite objectives is used to determine the compromise solutions between maximum output and minimal stack size. The obtained results are in good agreement with available literature data

Keywords—Biphasic model, PEM fuel cell, optimization, simulation, specie transport.

I. INTRODUCTION

IN stationary applications and transportation, PEM fuel cells have to reach efficiency equal or than 40%. However, because the efficiency decreases as the output power increases [1], i.e. to reach a great power, they require more energy consumption in auxiliaries systems. Since early models of [2] and [3] until lately model which consider only mono-phase flow, they give an acceptable approximation in limited current density interval. The tendencies are directed towards the biphasic models like that used by [4] and [5], but generally these models are more complicated and need high computing capacity. The present model is less complicated which is based on the study developed and validated by [6]. In addition to the assumptions enumerated in [6], this model does not take account of flow space variations. Moreover, the water balance was modified, so that it will be valid when liquid water and vapour are presents. The first step consists with model derivation which is used for optimization. This model should be precise, while choosing the reduced form in order to take account of repeated calculations to lead an optimal solution.

II. MATHEMATICAL PROCEDURES

A. Mass Balance

Fig. 1 shows an elementary PEM fuel cell with parallel gas channels at anode and cathode. This cell is composed of collector plate, gas diffusion layer (GDL) and catalyst layer at

both side of anode and cathode. The polymeric membrane is sandwiched in the center.

In this reduced fuel cells model, we neglect variables space dependency in flow channels. Essentially, we control vapor, liquid water and gases flows. Consequently, governing differential equations will be reduced to algebraic equations. For a given current density, hydrogen and oxygen mass balances are calculated using the difference between inlet flow and consumed flow by the chemical reaction:

Hydrogen mass balance:

$$M_{H_2} = M_{H_2,in} - \frac{AI}{2F} \quad (1)$$

Oxygen mass balance:

$$M_{O_2} = M_{O_2,in} - \frac{AI}{4F} \quad (2)$$

Nitrogen is assumed as inert gas, so does not participate in chemical reaction, i.e. inlet flow is equal to outlet flow:

$$M_{N_2} = M_{N_2,in} \quad (3)$$

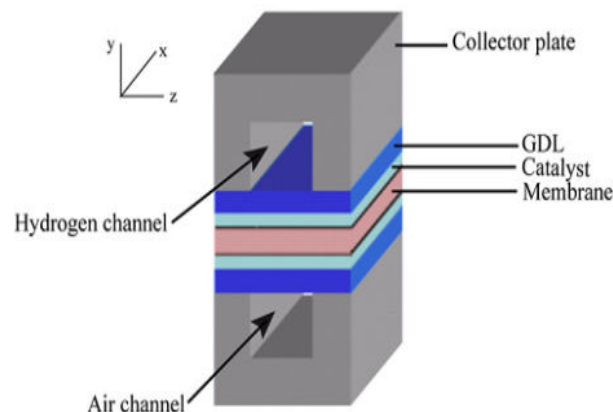


Fig. 1 Schematic of fuel cell

In channels, inlet reactant flows are determined according to consumed flows by chemical reaction and stoichiometric ratio. Hydrogen and oxygen flows are respectively expressed as:

$$M_{H_2,in} = \xi_{H_2} \frac{AI}{2F} \quad (4)$$

$$M_{O_2,in} = \xi_{Air} \frac{AI}{4F} \quad (5)$$

Water flows with presence of both vapor and liquid water are affected by the following factors [4], [5], [7]-[9]:

Boubekeur Dokkar, Nasreddine Chennouf, Noureddine Settou, Belkhir Negrou are with the Laboratoire de Valorisation et Promotion des Ressources Sahariennes, University of Kasdi Merbah, BP 511 Route Ghardaia 30000 Ouargla Algeria (phone: 213 7 75908983; corresponding e-mail: Boubekeur.ogx@gmail.com).

Abdesslam Benmhidi is with the Linde Gas Algeria, centre of Ouargla, 30000 Ouargla, Algeria. (e-mail: Abdesslem.benmhidi@linde.com).

- In cathode, water production by electrochemical reaction,
- Water transport from anode to cathode by electro-osmosis drag.
- Upstream water diffusion from cathode toward anode.
- Condensation and evaporation of water.

In anode side, water balance is formulated by (4) which shows that inlet water vapor in anode channel exhausts as vapor or condensed liquid or passes across membrane to the cathode:

$$M_{w,a}^V = M_{w,a,in}^V - M_{w,a}^l - \alpha \frac{AI}{F} \quad (6)$$

with α is net water molecules ratio passes across the membrane reported to protons flux.

In fuel cells operation, there are two cases which present at anode channel:

First case: if both liquid and vapor phases of water are present in anode channel, i.e. $M_{w,a}^l \neq 0$, as steady state is considered the equilibrium between liquid water and vapor is established, so water vapor is saturated and outlet vapor flow is expressed as:

$$M_{w,a}^V = M_{H_2} \frac{p_w^{sat}}{p - p_w^{sat}} \quad (7)$$

Outlet liquid water from anode channel, $M_{w,a}^l$, is the difference between inlet and outlet flows which is expressed by the following equation:

$$M_{w,a}^l = M_{w,a,in}^V - M_{w,a}^V - \alpha \frac{AI}{F} \quad (8)$$

Second case: if liquid water doesn't exist in anode channel, i.e. $M_{w,a}^l = 0$, so there isn't equilibrium between liquid and vapor phases. Outlet vapor $M_{w,a}^V$ is calculated as follow:

$$M_{w,a}^V = M_{w,a,in}^V - \alpha \frac{AI}{F} \quad (9)$$

As the same method, we analyze the situation at cathode side, so water balance in this channel takes account for outlet flows of vapor and liquid water, water vapor coming from anode to cathode and water produced by electrochemical reaction at cathode. The overall balance at cathode is expressed as follow:

$$M_{w,c}^V = M_{w,c,in}^V - M_{w,c}^l + \alpha \frac{AI}{F} + \frac{AI}{2F} \quad (10)$$

First case: if both liquid and vapor phases of water are present in cathode channel, i.e. $M_{w,c}^l \neq 0$, so water vapor is saturated and outlet vapor flow is expressed as:

$$M_{w,c}^V = (M_{O_2} + M_{N_2}) \frac{p_w^{sat}}{p - p_w^{sat}} \quad (11)$$

Outlet liquid water from cathode channel, $M_{w,c}^l$, is the difference between inlet and outlet flows which is expressed by the following equation:

$$M_{w,c}^l = M_{w,c,in}^V - M_{w,c}^V + \alpha \frac{AI}{F} + \frac{AI}{2F} \quad (12)$$

Second case: if liquid water doesn't exist in cathode channel, i.e. $M_{w,c}^l = 0$, so there isn't equilibrium between liquid and vapor phases. Outlet vapor $M_{w,c}^V$ is calculated as follow:

$$M_{w,c}^V = M_{w,c,in}^V + \alpha \frac{AI}{F} + \frac{AI}{2F} \quad (13)$$

Inlet water vapor at anode channel is calculated according to hydrogen relative humidity:

$$M_{w,a,in}^V = \frac{y_{w,a,in}}{1 - y_{w,a,in}} M_{H_2,in} \quad (14)$$

$$y_{w,a,in} = RH_{fuel} \frac{p_w^{sat}}{P} \quad (15)$$

Also, inlet water vapor at cathode channel is calculated according to air relative humidity:

$$M_{w,c,in}^V = \frac{y_{w,c,in}}{1 - y_{w,c,in}} M_{Air,in} \quad (16)$$

$$y_{w,c,in} = RH_{Air} \frac{p_w^{sat}}{P} \quad (17)$$

with $y_{w,a,in}$ and $y_{w,c,in}$ are respectively vapor molar fractions for inlet humid gas at anode and cathode channels, P is the pressure of gas vapor mixture in channels.

Vapor saturated pressure (atm) is expressed according to temperature (T °C) as follow [10]:

$$P_w^{sat} = 10^{-2.18 + 2.95 \cdot 10^2 T - 9.18 \cdot 10^{-5} T^2 + 1.44 \cdot 10^{-7} T^3} \quad (18)$$

For determining fuel cells outlet flows, we should calculate the coefficient α which represents the net ratio of water molecules passes across the membrane. It is the difference between coefficients of electro-osmotic drag and back diffusion of concentration gradient [2]:

$$\alpha = n_d - n_b$$

Electro-osmotic coefficient is expressed according to water activity:

$$n_d = 0.0049 + 2.024a - 4.53a^2 + 4.09a^3$$

Water activity at anode and cathode are obtained respectively by the following relations [10]:

$$a_a = \left(\frac{M_{w,a}^V}{M_{w,a}^V + M_{H_2}} \right) \frac{P}{p_w^{sat}}$$

$$a_c = \left(\frac{M_{w,c}^V}{M_{w,c}^V + M_{O_2} + M_{N_2}} \right) \frac{P}{p_w^{sat}}$$

Back diffusion coefficient of water concentration gradient is given by D. Bernardi et al. [3]:

$$n_b = \frac{F}{I} D_w \frac{(c_{w,c} - c_{w,a})}{t_m}$$

Diffusion coefficient in the membrane is expressed as [9]:

$$D_w = n_d D_0 \exp \left[2416 \left(\frac{1}{303} - \frac{1}{273 + T} \right) \right]$$

Water concentrations at anode and cathode membrane interfaces are expressed by the following relations [10]:

$$c_{w,a} = \frac{\rho_{m,dry}}{M_{m,dry}} (0.300 + 10.8a_a - 16.0a_a^2 + 14.1a_a^3)$$

$$c_{w,c} = \frac{\rho_{m,dry}}{M_{m,dry}} (0.300 + 10.8a_c - 16.0a_c^2 + 14.1a_c^3)$$

with $\rho_{m,dry}$ and $M_{m,dry}$ are respectively density and molar mass of dry membrane.

We note that coefficient α depends on water vapor flows which in turn depend on this coefficient. So, the coefficient calculation requires the resolution of an implicit equation $\alpha = g(\alpha)$.

B. Fuel Cell Electrochemistry

Fuel cells effective voltage is expressed as the difference between reversible thermodynamic voltage and different overvoltage losses:

$$V_{cel} = V_{rev} - V_{act} - V_{ohm} - V_{con} \quad (19)$$

Reversible thermodynamic voltage: this voltage is based on Nernst equation [9]:

$$V_{rev} = V_{oc} + \frac{R(273 + T)}{2F} \ln \left(\frac{P_{H_2} P_{O_2}^{0.5}}{P_{H_2O}} \right)$$

with V_{oc} is open circuit voltage.

Activation overvoltage represents loss due to reaction rate at electrodes surface, this overvoltage is assumed that mainly occurs at cathode side [9]:

$$V_{act} = \frac{R(273 + T)}{0.5F} \ln \left(\frac{I}{I_0 P_{O_2}} \right)$$

with V_{oc} is open circuit voltage.

Ohmic overvoltage represents voltage loss due to resistance against protons flow in the electrolyte [9]:

$$V_{ohm} = \frac{I t_m}{\sigma_m}$$

with t_m is the membrane thickness,

Membrane resistance σ_m is expressed as follow [10]:

$$\sigma_m = \left(0.00514 \frac{M_{m,dry}}{\rho_{m,dry}} \lambda_m - 0.00324 \right) \exp \left\{ 1268 \left(\frac{1}{303} - \frac{1}{273 + T} \right) \right\}$$

with λ_m is membrane water content.

In literature, we find different approaches used for determining membrane water content. Golbert et al. [8] take it as anode water content, L. Wang et al. [11] calculate with the same value at cathode and Pukrushpan [7] use mean activity value between anode and cathode. In this work, we adopt the last approach:

$$a_m = \frac{a_a + a_c}{2}$$

Water content is expressed as the relation given by Springer et al. [2]:

$$\lambda_m = 0.043 + 17.81a_m - 39.85a_m^2 + 36.0a_m^3$$

Concentration overvoltage represents voltage loss due to mass transport limitation [12]:

$$V_{con} = \beta I^K \ln \left(\frac{I_L}{I_L - I} \right)$$

With βI^K is mass transport amplification term linked with the overvoltage, expressed as voltage unity, and I_L is limiting current density.

With substituting precedent terms in (19) we obtain the expression of cell voltage:

$$V_{cel} = V_{oc} + \frac{R(273 + T)}{2F} \ln \left(\frac{P_{H_2} P_{O_2}^{0.5}}{P_{H_2O}} \right) - \frac{R(273 + T)}{0.5F} \ln \left(\frac{I}{I_0 P_{O_2}} \right) - \frac{I t_m}{\sigma_m} - \beta I^K \ln \left(\frac{I_L}{I_L - I} \right) \quad (20)$$

C. System Efficiency

For evaluating the performance of fuel cells stack, generally we use the efficiency as indicator. System efficiency is defined as the ratio between stack net output power and self fuel heating:

$$\eta = \frac{W_{stack} - W_{prs}}{W_{fuel}} \quad (21)$$

Self fuel heating:

$$W_{stack} = n_{cel} \xi_{H_2} \frac{AI}{4F} LHV \quad (22)$$

with LHV is lower heating value of hydrogen, and n_{cel} is number of cells. In calculation we take $n_{cel} = 11$, so the area A represents all MEA active area.

Stack output power [13]:

$$W_{stack} = n_{cel} A I V \quad (23)$$

Parasitic power is the sum of consumed power by air compressor and others accessories as humidifiers and cooling system [13]:

$$W_{prs} = W_{comp} + W_{others} \quad (24)$$

Consumed power by air compressor W_{comp} [13]:

$$W_{comp} = \frac{c_p T_e}{\eta_c \eta_{mt}} \left\{ \left(\frac{P}{P_{in}} \right)^{0.286} - 1 \right\} m_{air} \quad (25)$$

with m_{air} is air mass flow [13]:

$$m_{air} = 3.57 * 10^{-7} n_{cel} \xi_{air} A I \quad (26)$$

Others power losses W_{others} are taken by Pei et al. [14] equal to 2 kW based on output fuel cells of 62.5 kW. Instead of this value, we assumed W_{others} as 5% of stack nominal output power. Efficiencies of compressor and electric motor are constants, as the approach adopted by others authors [13]:

$$W_{others} = 0.05 W_{stack} \quad (27)$$

D. System Optimization

The approach presented in our previous work [15] shows that PEM fuel cells size (MEA active area) and system efficiency are two opposed objectives which should be optimized. The first objective function (MEA total active area) should be minimized, but the second objective function (system efficiency) should be maximized. Multi-objective optimization is equivalent to resolve the problem defined as follow:

$$\begin{cases} \min f_1(x), & x \in R^6 \\ \max f_2(x), & x \in R^6 \\ x_k \min \leq x_k \leq x_k \max & k = 1, \dots, 6 \end{cases}$$

with function f_1 is active area "A"

Function f_2 is efficiency "η"

The variables are:

- x_1 : current density "i"
- x_2 : cells pressure "P"
- x_3 : hydrogen stoichiometric ratio " ξ_{H_2} "
- x_4 : air stoichiometric ratio " ξ_{Air} "
- x_5 : hydrogen relative humidity " RH_{H_2} "
- x_6 : air relative humidity " RH_{Air} "

The goal of this optimization is to find solutions which represent a compromise between efficiency and size in order to realize conception of PEM fuel cells system for insuring required power. Optimal solutions set present a compromise between two objectives, is called Pareto set. Weighting method is adopted for determining this Pareto set.

The variables bounds are fixed according to common values used in practice [9]-[13]. Bounds of air relative humidity are taken from meteorological statistics of Ouargla city (in south of Algeria). Superior bound of hydrogen relative humidity is lightly reduced. Variables bounds became as follow:

$$\begin{aligned} 0.11 &\leq x_1 \leq 1.3 \\ 1.2 &\leq x_2 \leq 5 \\ 1.1 &\leq x_3 \leq 10 \\ 1.1 &\leq x_4 \leq 10 \\ 0.25 &\leq x_5 \leq 0.60 \\ 0.50 &\leq x_6 \leq 0.80 \end{aligned}$$

III. NUMERICAL PROCEDURES

Calculation Steps start by the determination of inlet reactants flows. Furthermore, the calculation of outlet flows with corresponding voltages. Numerical solution of governing equations is calculated by Matlab program and the optimization is achieved using "Toolbox". Genetic algorithm method (GA) is chosen for program execution. For each introduced ω value, obtained solution is taken as initial point for continuing program execution with Qasi-Nexton method. Computing precision is fixed at relative error of 1.e-5. Physical parameters used in the model and base case conditions are presented in Table I.

TABLE I
PARAMETERS AND BASE CASE CONDITIONS [9]

Designation	Value	Unity
Amplification constant (β)	0.085	V/cm ² A ⁻¹
Exponent of amplification constant (k)	1.1	
Density of limiting current (I_L)	1.4	Acm ⁻²
Lower heating value of hydrogen (LHV)	24 x 10 ⁵	Jmol ⁻¹
Exchange current density at cathode (I_0)	0.01	Acm ⁻²
Open circuit voltage (V_{oc})	1.1	V
Coefficient of water diffusion in the membrane (D_0)	5.5 x 10 ⁻⁷	cm ² s ⁻¹
Density of dry membrane ($\rho_{m,dry}$)	2	gcm ⁻³
Molar mass of dry membrane ($M_{m,dry}$)	1100	gmol ⁻¹
Membrane thickness (t_m)	5 x 10 ⁻³	cm
Compressor efficiency (η_c)	0.85	
Compressor inlet temperature (T_e)	15 °C	°C
Compressor inlet pressure (P_m)	1	atm
Electric motor efficiency (η_m)	0.85	
Calorific capacity of air (c_p)	1004	JK ⁻¹ kg ⁻¹
Operating temperature (T)	80	°C
Relative humidity at anode /cathode (RH)	100/50	%
Stoichiometric ratio at anode /cathode (ξ)	1.25/2	
Cells pressure (P)	2	atm

IV. RESULTS AND DISCUSSIONS

A. Effect of Operating Pressure

Fig. 2 shows the effect of operating pressure variation on polarization curves. At high current density, these curves record important fall which take the same shapes as experimental data given by L. Wang et al. [11]. We note that on one hand, voltage decreases when current density increase due to overvoltage mentioned previously in section II. On the other hand, power density (voltage*current density) increases according to current density until reaching its maximum at relatively high current density. In addition, polarization curves show that voltage increases with pressure rise. However, the pressure hasn't a significant effect on system efficiency because any voltage increase will be penalized by parasitic power rise, which in turn increase according to pressure. The obtained results are in good agreement with the work of Sheila et al. [9].

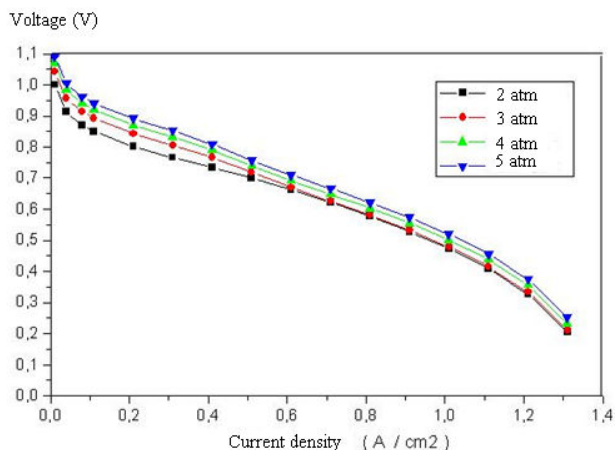


Fig. 2 Effect of pressure on polarization curve

B. Curve of Pareto Set

Fig. 3 shows optimal solutions for 50 kW PEM fuel cells. Base case solution (green point) is inside the convex space limited by Pareto curve, therefore this point represents a dominated situation. Optimal solutions are compromise solutions between the efficiency and MEA active area. The curve is composed of all designs which are optimal in the Pareto sense. The highest point (in top on the right) in Fig. 3 represents the optimal solution for $\omega=1$, which corresponds to the problem with simple optimization objective which consists in maximizing the output of the system without taking account of stack size. This solution is 23% more efficient but the size is 107% larger than the base case. This design requires operation with low current density (thus, at higher voltage), with higher pressure, and with small hydrogen and air stoichiometric ratios compared to the base case. Consequently, it reaches higher efficiency with low fuel consumption. However, the parasitic loss is higher due to pressure increase.

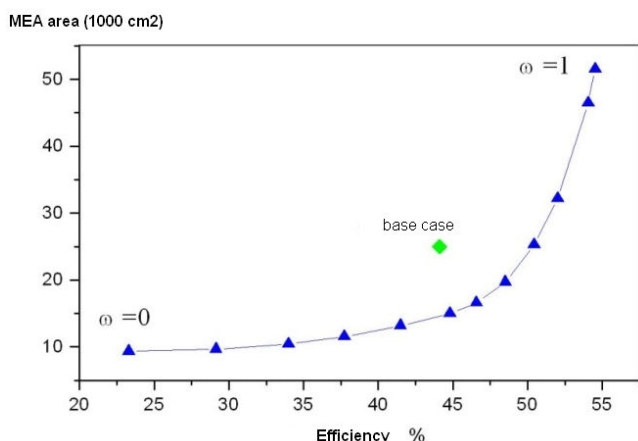


Fig. 3 Pareto set and base case

C. Objectives Evolution

The optimal values of relative humidity and hydrogen stoichiometric ratio are 0.8 and 1.1 respectively, remaining without variation for all ω weights.

Fig. 4 shows optimal values of the objectives according to current density. At low current densities, we note that solutions which have big size and high efficiency form the branches at right-hand sides. Conversely, left branches contain the solutions which are characterized by small size and low efficiency, corresponding to high current density. Generally, according to current density, MEA area, stack efficiency and voltage decrease.

During optimization, some variables bounds are violated particularly lower bound of current density, pressure upper bound, and hydrogen stoichiometric ratio bounds. Concerning lower bounds of current density and hydrogen stoichiometric ratio, we note that current density less than 0.11 and hydrogen stoichiometric ratio less than 1.1. A cm^2 are not used in practice.

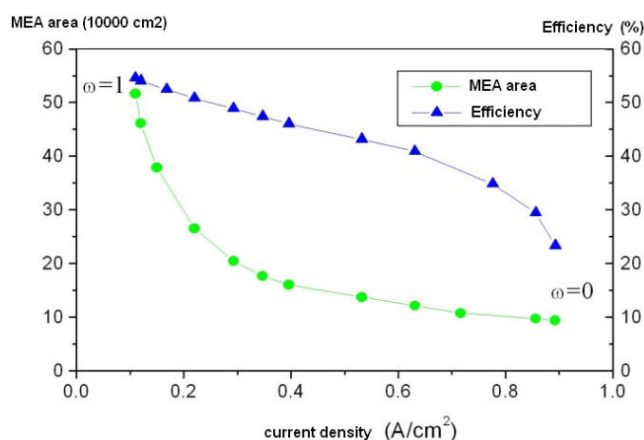


Fig. 4 Objectives evolution

V. CONCLUSION

In contrary of monophasic model given in our previous work [16], we note that cells voltage in this biphasic model records very important fall at high current density to behave as the experimental polarization curve

Optimization stochastic method is used in this complicated objective function to reach the global minima. But, it requires refining operation by deterministic method. The obtained results indicate that output and stack size are opposed objectives, because for reaching high efficiency, the system must operate at low current density. The low current density coincides with low power density that means we need a greater system characterized by wide area to improve stack power. An optimization study is carried out to examine at which operating pressure level and until which humidification reduction we can go down, in order to have high power and low parasitic consumption (humidifiers, pump, compressor,...).

REFERENCES

- [1] J. Larminie, A. Dicks, Fuel Cell Systems Explained, Wiley, New York, 2002.
- [2] Springer, T. E.; T.A. Zawodzinski, S. Gottesfeld, Polymer electrolyte fuel cell model. J. Electrochem. Soc. 138(8), 1991, pp. 2334-2342.
- [3] D.M. Bernardi, M.W. Verbrugge, Mathematical model of the solid polymer-electrolyte fuel cell. J. Electrochem. Soc.; 139 (9), 1992, pp. 2477-2491.

- [4] N.P. Siegel, M.W. Ellis, D.J. Nelson, M.R. von Spakovsky, A two-dimensional computational model of a PEMFC with liquid water transport. *Journal of Power Sources*; 128, 2004, pp. 173–184.
- [5] Yun Wang, Chao-Yang Wang. A Nonisothermal, Two-Phase Model for Polymer Electrolyte Fuel Cells. *Journal of the Electrochemical Society*; 153(6), 2006, pp. A1193-A1200.
- [6] T.V. Nguyen, R.E. White, *Journal of the Electrochemical Society* 140 (8), 1993, pp. 2178–2186,
- [7] Jay Tawce Pukurshpan, Modelling and control of fuel cell systems and fuel processors, Phd Thesis of mechanical engineering, University of Michigan, USA, 2003.
- [8] J. Golbert, D.R. Lewin, Model-based control of fuel cells (2): Optimal efficiency, *Journal of Power Sources* 173, 2007, pp. 298–30.
- [9] Sheila Mae C. Anga,b, Daniel J.L. Bretta, Eric S. Fraga, A multi-objective optimisation model for a general polymer electrolyte membrane fuel cell system, *Journal of Power Sources* 195, 2010, pp. 2754–2763.
- [10] J. Golbert, D.R. Lewin, *Journal of Power Sources* 135 (1–2) , 2004, pp. 135–151
- [11] Wang L., Husar A., Zhou T., Liu H., A parametric study of PEM fuel cell performances. *International Journal of Hydrogen Energy* 28, 2003, pp. 1263-1272.
- [12] G. Squadrito, G. Maggio, E. Passalacqua, F. Lufrano, A. Patti, *Journal of Applied Electrochemistry* 29 (12) , 1991, pp.1449–1455
- [13] Woonki Na, Bei Gou, The efficient and economic design of PEM fuel cell systems by multi-objective optimization, *Journal of Power Sources* 166, 2007, pp. 411–418.
- [14] P. Pei, W. Yang, P. Li, *International Journal of Hydrogen Energy* 31, 2006, pp. 361–369.
- [15] B. Dokkar, N. Settou, O. Imine, B. Negrou, N. Chennouf, A. Benmhidi, "Analyse et simulation d'un modèle diphasique d'une pile à combustible PEMFC", *Proceeding ICER 2012 Bejaia, Algeria*
- [16] B. Dokkar, N. Settou, O. Imine, N. Saifi, B. Negrou, Z. Nemouchi, "Simulation of species transport and water management in PEM fuel cells", *International Journal of Hydrogen Energy*, volume 36 issue 6, 2011, pp. 4220-4227.